Supporting Information for

Is strong axial crystal-field the only essential condition for large magnetic anisotropy barrier? Case of non-Kramers Ho(III) versus Tb(III)

Sandeep K. Gupta, Thayalan Rajeshkumar, Gopalan Rajaraman and Ramaswamy Murugavel

Department of Chemistry, Indian Institute of Technology Bombay, Mumbai-400076, India.

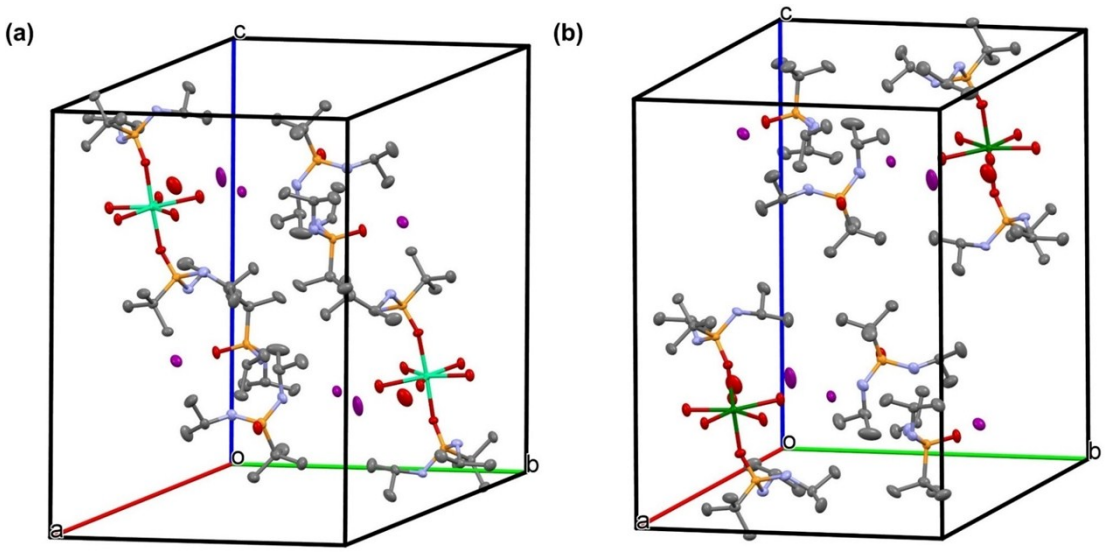

Figure S1. Unit cell packing diagram of (a) **1** and (b) **2**. Hydrogen atoms have been omitted for clarity.

Table S1. Selected bond distances (Å) and angles (°) in compound **1**.

Ho(1)-O(1)	2.192(2)	O(1)-Ho(1)-O(5)	85.78(10)	O(5)-Ho(1)-O(6)	70.53(10)
Ho(1)-O(2)	2.196(2)	O(1)-Ho(1)-O(6)	91.97(10)	O(5)-Ho(1)-O(7)	141.88(10)
Ho(1)-O(5)	2.335(3)	O(1)-Ho(1)-O(7)	92.70(10)	O(5)-Ho(1)-O(9)	73.34(10)
Ho(1)-O(6)	2.346(3)	O(1)-Ho(1)-O(8)	88.24(10)	O(6)-Ho(1)-O(9)	143.63(10)
Ho(1)-O(7)	2.342(2)	O(1)-Ho(1)-O(9)	89.38(10)	O(7)-Ho(1)-O(6)	71.47(9)
Ho(1)-O(8)	2.334(3)	O(2)-Ho(1)-O(5)	89.56(10)	O(7)-Ho(1)-O(9)	144.78(10)
Ho(1)-O(9)	2.358(3)	O(2)-Ho(1)-O(6)	87.98(10)	O(8)-Ho(1)-O(5)	144.81(10)
O(1)-Ho(1)-O(2)	175.07(9)	O(2)-Ho(1)-O(7)	91.96(10)	O(8)-Ho(1)-O(6)	144.42(10)
P(1)-O(1)-Ho(1)	155.22(16)	O(2)-Ho(1)-O(8)	94.66(10)	O(8)-Ho(1)-O(7)	72.98(10)
P(2)-O(2)-Ho(1)	149.86(15)	O(2)-Ho(1)-O(9)	87.74(10)	O(8)-Ho(1)-O(9)	71.94(10)

Table S2. Selected bond distances (Å) and angles (°) in compound **2**.

O(1)-Tb(1)	2.230(2)	O(1)-Tb(1)-O(5)	87.28(10)	O(5)-Tb(1)-O(7)	143.90(10)
O(2)-Tb(1)	2.224(2)	O(1)-Tb(1)-O(6)	89.09(10)	O(6)-Tb(1)-O(5)	70.66(10)
O(5)-Tb(1)	2.386(3)	O(1)-Tb(1)-O(7)	88.11(10)	O(6)-Tb(1)-O(7)	73.48(10)
O(6)-Tb(1)	2.370(3)	O(1)-Tb(1)-O(8)	95.62(11)	O(6)-Tb(1)-O(8)	144.72(10)
O(7)-Tb(1)	2.397(3)	O(1)-Tb(1)-O(9)	91.95(10)	O(6)-Tb(1)-O(9)	142.05(10)
O(8)-Tb(1)	2.373(3)	O(2)-Tb(1)-O(5)	92.57(10)	O(8)-Tb(1)-O(5)	144.33(10)
O(9)-Tb(1)	2.376(3)	O(2)-Tb(1)-O(6)	85.84(10)	O(8)-Tb(1)-O(7)	71.77(10)
O(2)-Tb(1)-O(1)	174.67(9)	O(2)-Tb(1)-O(7)	88.88(10)	O(8)-Tb(1)-O(9)	72.88(10)
P(1)-O(1)-Tb(1)	149.88(16)	O(2)-Tb(1)-O(8)	87.62(11)	O(9)-Tb(1)-O(5)	71.50(10)
P(2)-O(2)-Tb(1)	155.01(17)	O(2)-Tb(1)-O(9)	93.05(10)	O(9)-Tb(1)-O(7)	144.47(10)

Table S3. SHAPE measures of seven coordinates relative to structures of Ln(III) complexes.

Shape	**Symmetry**	**Deviation**	
		1	**2**
Johnson elongated triangular pyramid	C_{3v}	23.073	22.802
Johnson pentagonal bipyramid	D_{5h}	2.705	2.712
Capped trigonal prism	C_{2v}	5.908	5.757
Capped octahedron	C_{3v}	7.756	7.625
Pentagonal bipyramid	$\boldsymbol{D_{5h}}$	**0.20**	**0.227**
Hexagonal pyramid	C_{6v}	24.633	24.485
Heptagon	D_{7h}	33.938	33.53

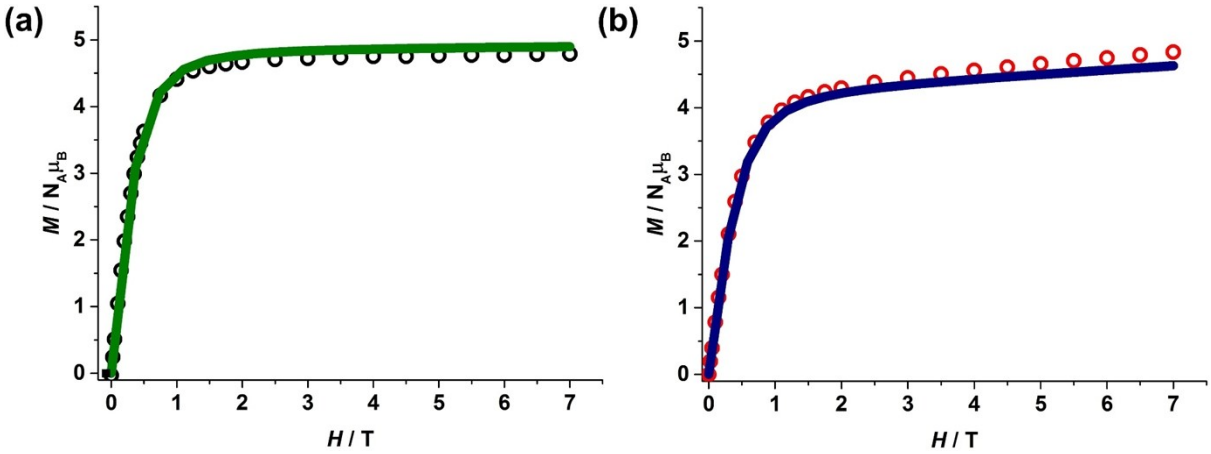

Figure S2. Field dependence of magnetization plot at 2K for (a) **1** and (b) **2**, respectively. The solid lines correspond to the computed magnetic susceptibilities from *ab initio* calculations.

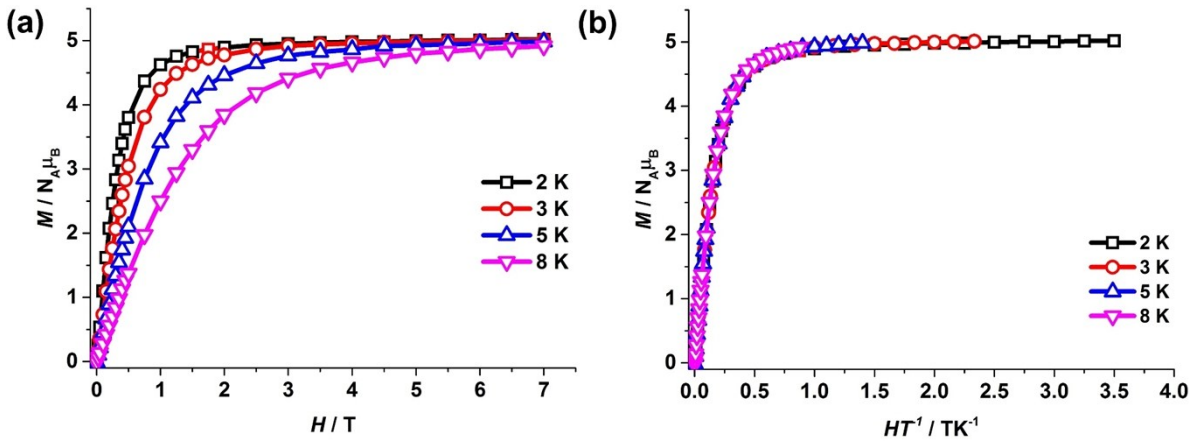

Figure S3. (a) Field dependence of magnetization and (b) the reduced magnetization plot for **1** at different temperatures. Solid lines are guides.

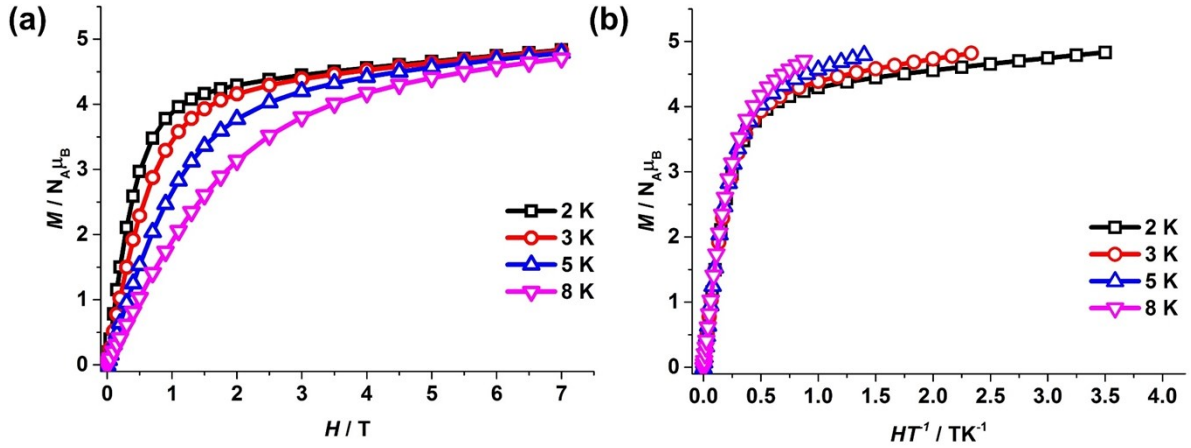

Figure S4. (a) Field dependence of magnetization and (b) the reduced magnetization plot for **2** at different temperatures. Solid lines are guides.

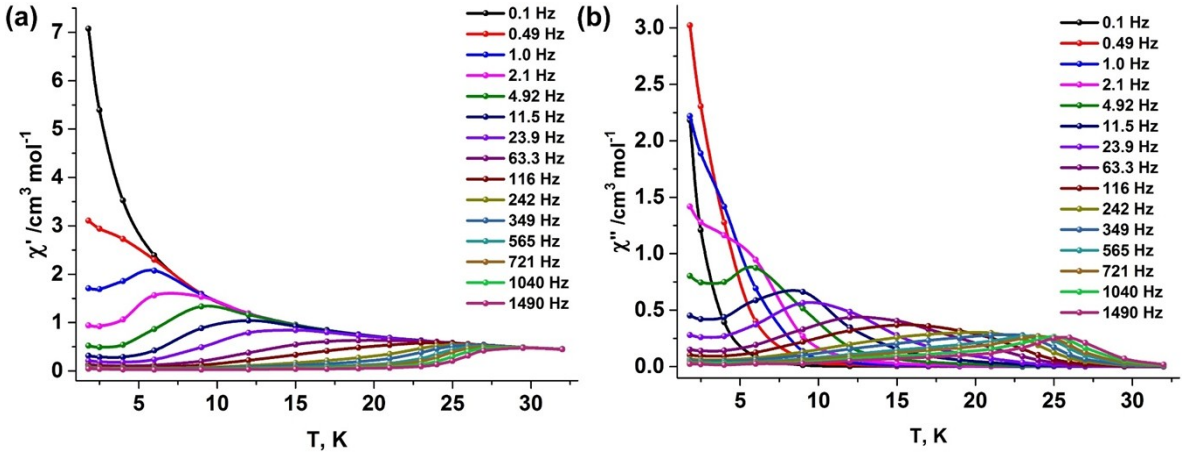

Figure S5. (a) In-phase (χ_M') component and (b) out-of-phase (χ_M'') component of the temperature dependent ac susceptibility for **1** measured in an oscillating ac field of 3.5 Oe and zero dc field.

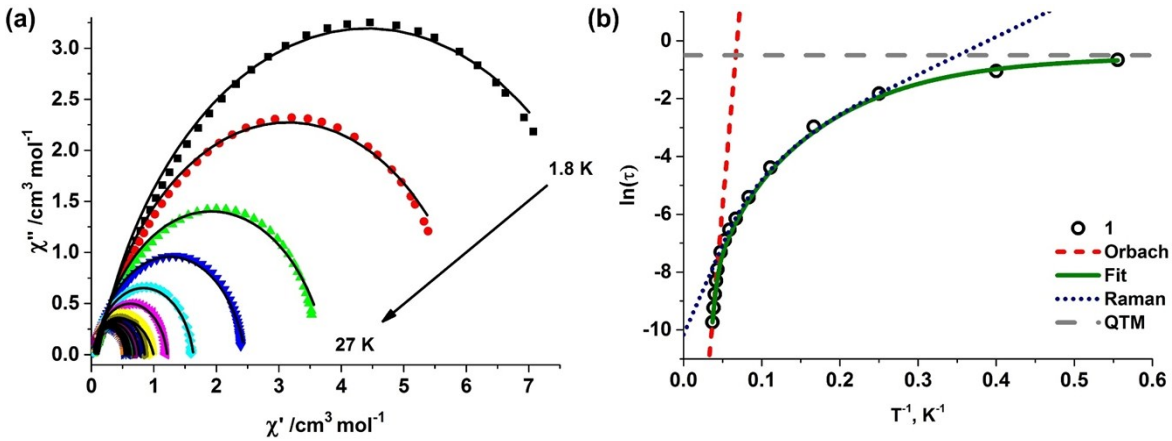

Figure S6. (a) Plots of χ_M'' vs χ_M' for **1** at zero dc field. Solid lines are the fits with the Debye functions. (b) Plot of the relaxation time τ (logarithmic scale) versus T^{-1} obtained; the solid red line corresponds to the best fitting to the multiple relaxation equation.

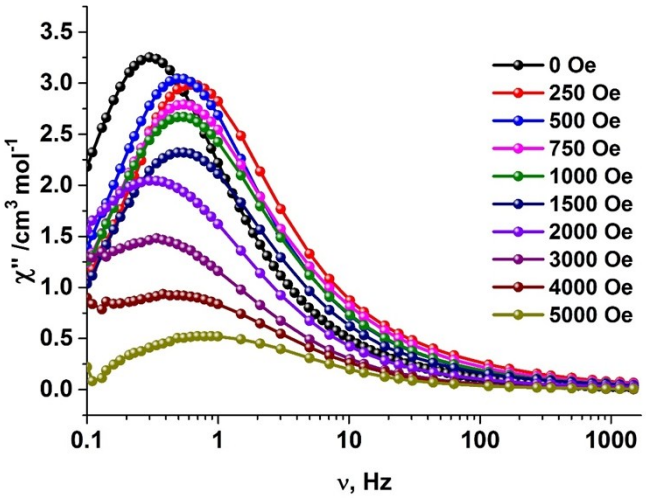

Figure S7. Frequency dependence of the out-of-phase (χ_M'') component of the ac susceptibility for **1** measured in an oscillating ac field of 3.5 Oe under various applied dc field.

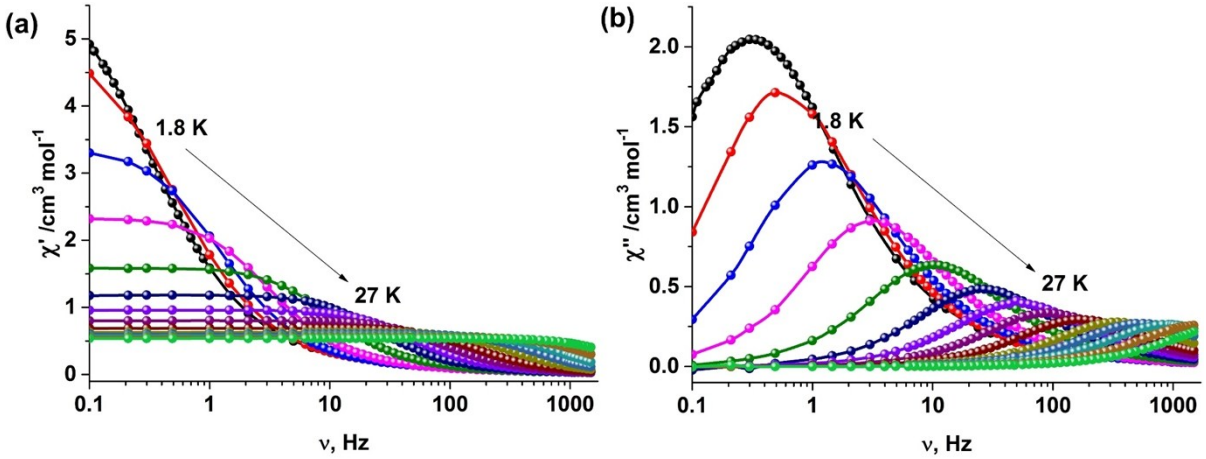

Figure S8. (a) In-phase (χ_M') component and (b) out-of-phase (χ_M'') component of the frequency dependent (0.1–1500 Hz) ac susceptibility for **1** measured in an oscillating ac field of 3.5 Oe and under an applied dc field of 2000 Oe.

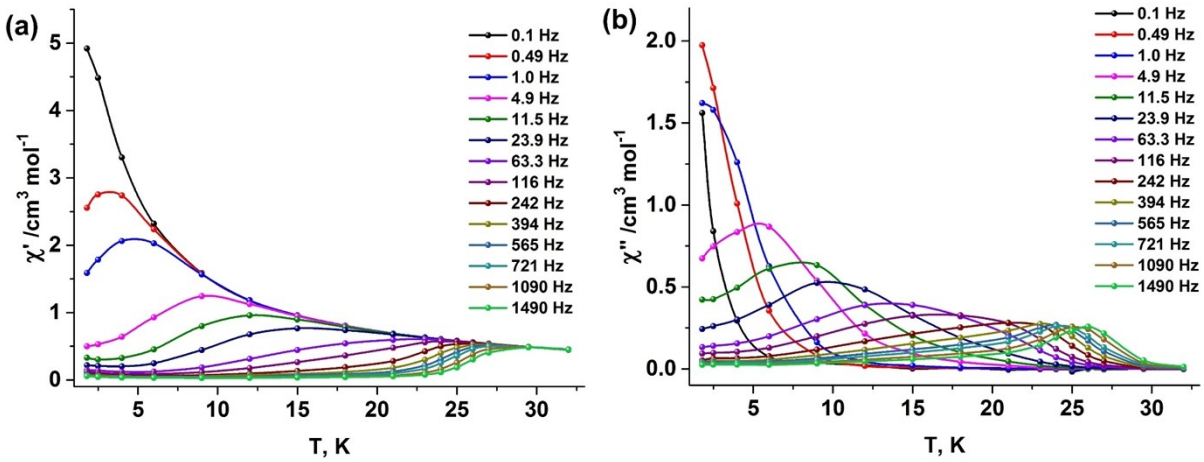

Figure S9. (a) In-phase (χ_M') component and (b) out-of-phase (χ_M'') component of the temperature dependent ac susceptibility for **1** measured in an oscillating ac field of 3.5 Oe and under an applied dc field of 2000 Oe.

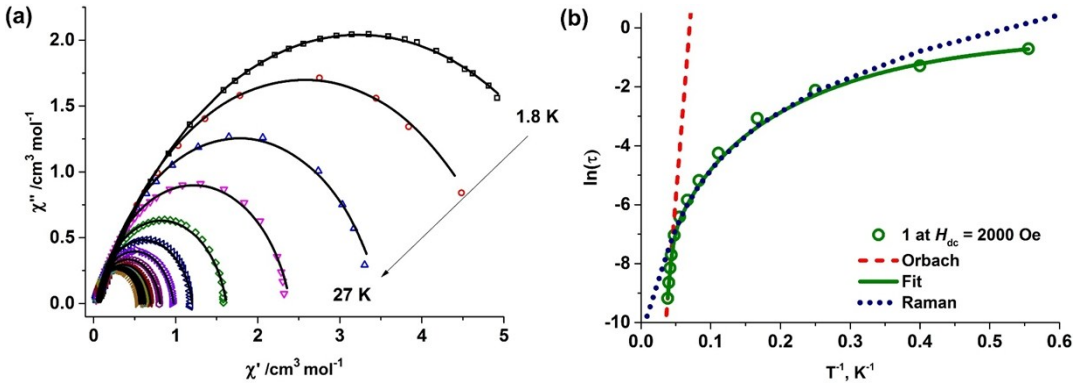

Figure S10. (a) Plots of χ_M'' vs χ_M' for **1** under an applied dc field of 2000 Oe. Solid lines are the fits with the Debye functions ($0.02 < \alpha < 0.27$). (b) Plot of the relaxation time τ (logarithmic scale) versus T^{-1} obtained; the solid red line corresponds to the best fitting to the multiple relaxation equation.

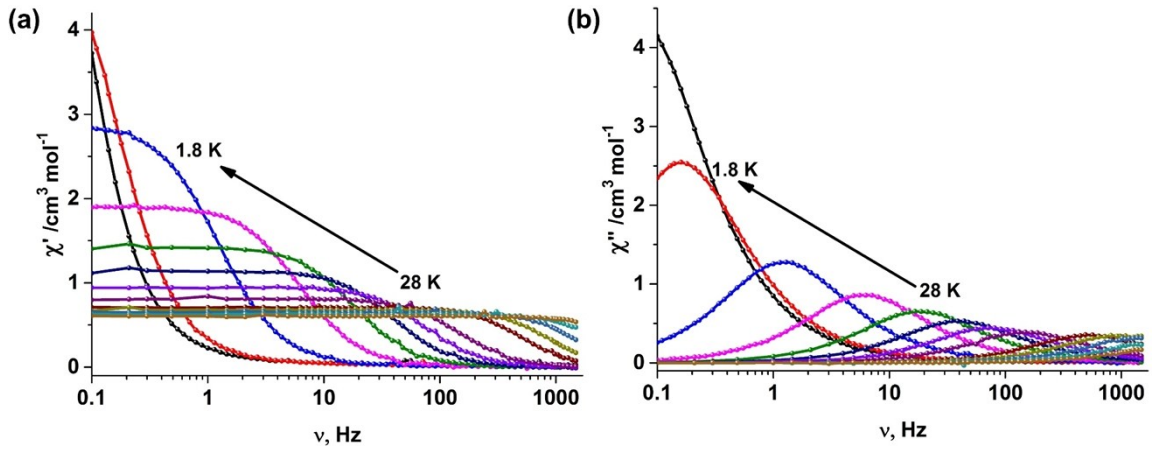

Figure S11. (a) In-phase (χ_M') component and (b) out-of-phase (χ_M'') component of the frequency dependent (0.1–1500 Hz) ac susceptibility for **1'** measured in an oscillating ac field of 3.5 Oe and zero dc field.

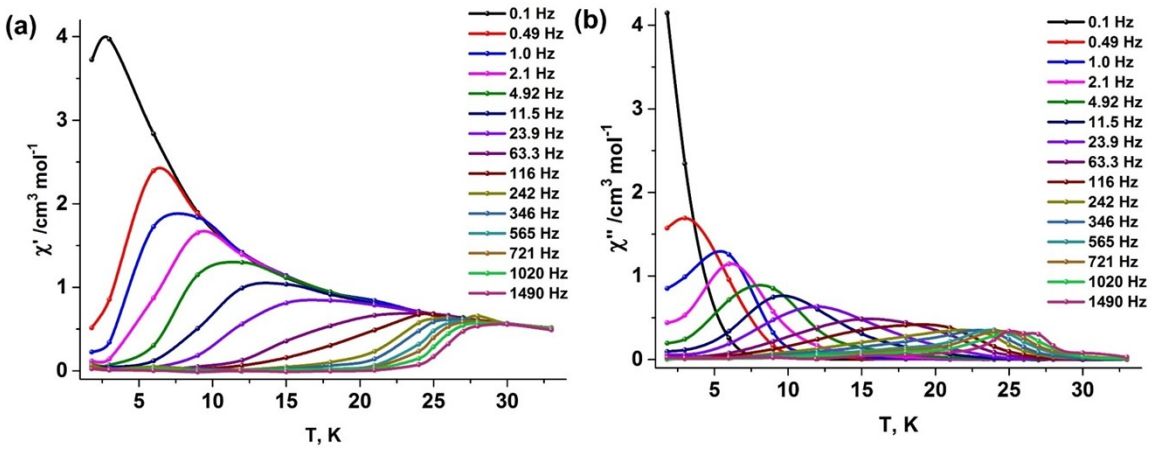

Figure S12. (a) In-phase (χ_M') component and (b) out-of-phase (χ_M'') component of the temperature dependent ac susceptibility for **1'** measured in an oscillating ac field of 3.5 Oe and under zero dc field.

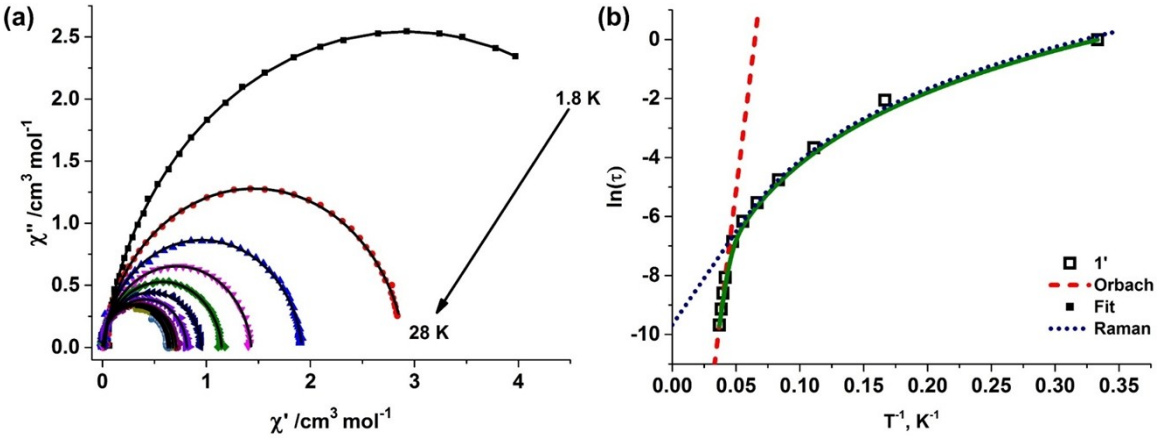

Figure S13. (a) Plots of χ_M'' vs χ_M' for **1'** at zero dc field. Solid lines are the fits with the Debye functions ($0 < \alpha < 0.08$) . (b) Plot of the relaxation time τ (logarithmic scale) versus T^{-1} obtained; the solid red line corresponds to the best fitting to the multiple relaxation equation ($C = 0.0215\ s^{-1}\ K^{-n}$ and $n = 3.5$).

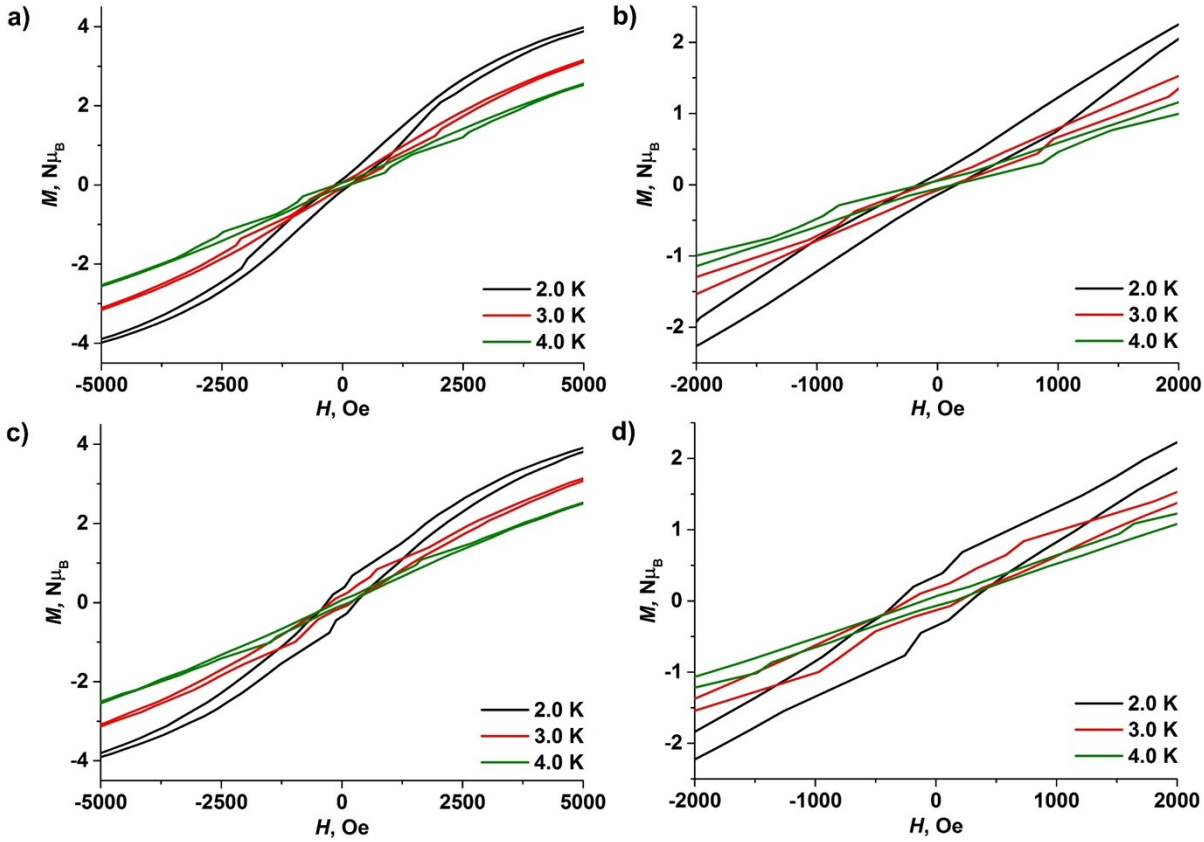

Figure S14. The field-dependent magnetization data for **1** (a & b) and **1'** (c & d)at a sweep rate of 0.027 T s^{-1}.

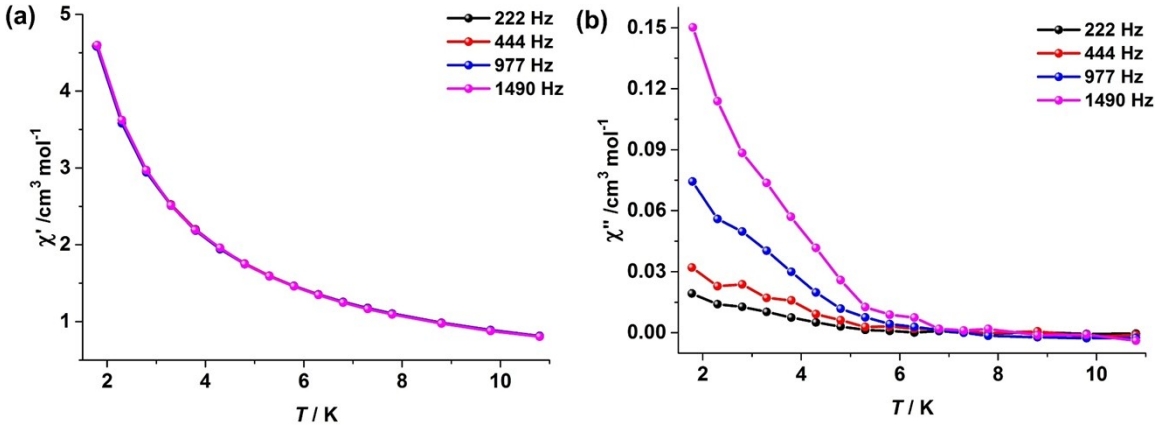

Figure S15. (a) In-phase (χ_M') component and (b) out-of-phase (χ_M) component of the temperature dependent ac susceptibility for **2** measured in an oscillating ac field of 3.5 Oe and under a zero dc field.

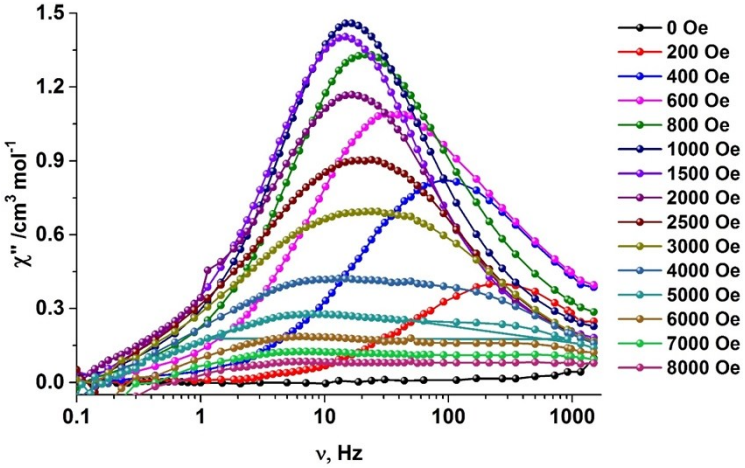

Figure S16. Frequency dependence of the out-of-phase (χ_M'') component of the ac susceptibility for **2** measured in an oscillating ac field of 3.5 Oe under various applied dc field.

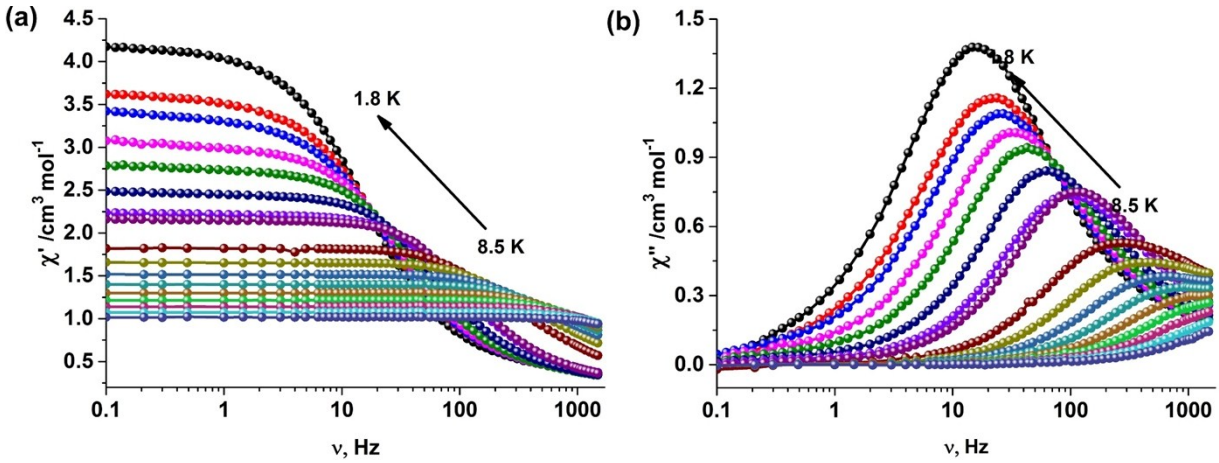

Figure S17. (a) In-phase (χ_M') component and (b) out-of-phase (χ_M⍰) component of the frequency dependent (0.1–1500 Hz) ac susceptibility for **2** measured in an oscillating ac field of 3.5 Oe and under an applied dc field of 1500 Oe.

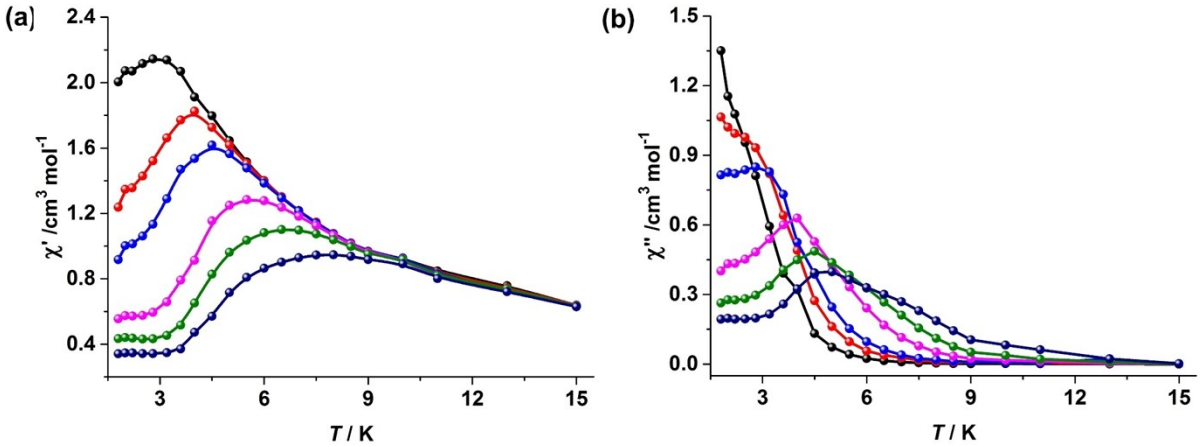

Figure S18. (a) In-phase (χ_M') component and (b) out-of-phase (χ_M⍰) component of the temperature dependent ac susceptibility for **2** measured in an oscillating ac field of 3.5 Oe and under an applied dc field of 1500 Oe.

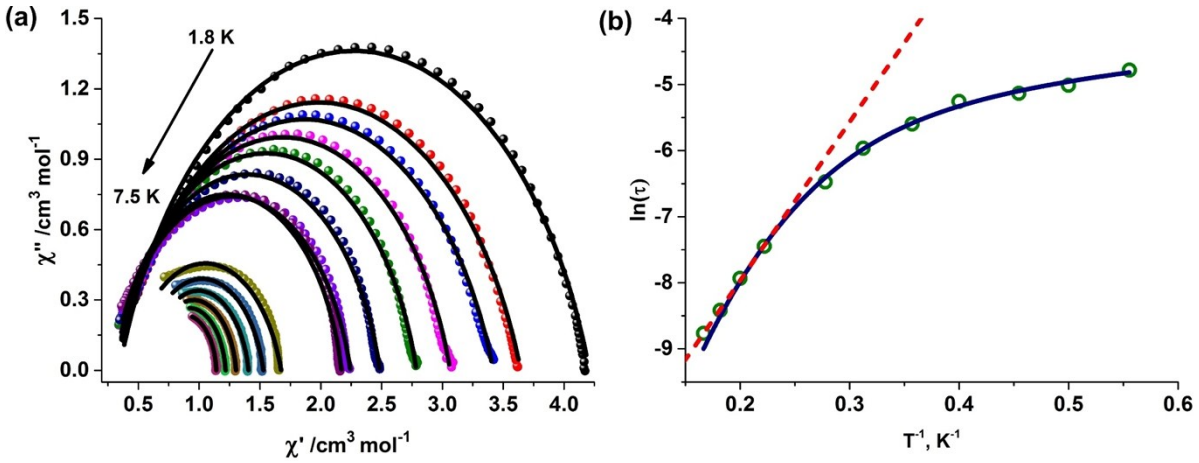

Figure S19. (a) Plots of χ_M⍰ vs χ_M' for **2** under an applied dc field of 1500 Oe. Solid lines are the fits with the Debye functions. (b) Plot of the relaxation time τ (logarithmic scale) versus T^{-1} obtained; the solid red line corresponds to the best fitting to the multiple relaxation equation (C = 0.83 s^{-1} K^{-n} and n = 5.04; τ_{QTM} = 0.0086 s^{-1}).

Table S4: SINGLE_ANISO computed spectrum, g tensors, relative energies and angles (q) of the principal anisotropy axes of the first excited states with respect to the ground state, for ground and excited state pseudo doublets of **1**

Levels	Energy (cm^{-1})	g_{zz}	Δ_{Tun}	Angles between *gzz* axis
1	0.000	19.85	0.001	–
2	0.001			
3	259.693	18.24	0.849	73.44
4	260.542			
5	284.263	16.04	1.262	5.43
6	285.525			
7	295.003	–	–	–
8	302.580	7.18	2.767	74.89
9	305.347			
10	308.583	–	–	–
11	317.193	–	–	–
12	328.023	12.11	6.115	55.22
13	334.138			
14	344.720	13.91	3.464	40.12
15	348.184			
16	359.788	14.99	1.571	18.93
17	361.359			

Table S5: Composition of wave functions of the ground J = 8 of Ho(III) for complex **1** as derived from SINGLE_ANISO calculations

w.f.	m_J	c_i		w.f.	m_J	c_i	
		real	imag			real	imag
1	-8	-0.677462	-0.200990	2	-8	-0.677464	-0.200990
	-7	0.000428	-0.001113		-7	0.000433	-0.001110
	-6	0.016091	0.008120		-6	0.016082	0.008116
	-5	0.011653	0.010925		-5	0.011642	0.010935
	-4	-0.003707	-0.002563		-4	-0.003551	-0.002335
	-3	0.003826	-0.001723		-3	0.004054	-0.001816
	-2	0.001397	0.005117		-2	0.001334	0.004971
	-1	-0.000391	0.000438		-1	-0.000328	-0.000168
	0	0.000085	-0.000586		0	-0.000090	-0.000013
	1	-0.000250	-0.000532		1	0.000362	-0.000068
	2	-0.002795	0.004509		2	0.002693	-0.004386
	3	0.003178	0.002740		3	-0.003371	-0.002894
	4	0.004283	-0.001403		4	-0.004069	0.001229
	5	0.014279	-0.007160		5	-0.014271	0.007172
	6	-0.017736	0.003208		6	0.017726	-0.003207
	7	0.000094	0.001189		7	-0.000100	-0.001188
	8	0.706648	0.000000		8	-0.706650	-0.000000
3	-8	-0.004425	-0.000533	4	-8	-0.004594	-0.000007
	-7	0.040743	0.033347		-7	0.060778	0.041310
	-6	-0.019157	0.008580		-6	-0.032192	0.011926
	-5	-0.121264	-0.025736		-5	-0.079823	-0.008485
	-4	-0.175290	-0.065271		-4	-0.280659	-0.158421
	-3	-0.315354	-0.369429		-3	-0.304554	-0.107776
	-2	-0.315953	-0.185765		-2	-0.199373	-0.370672
	-1	-0.029588	-0.198367		-1	-0.204310	-0.244602
	0	0.016067	-0.267578		0	0.001014	0.000001
	1	-0.053113	0.193401		1	0.204708	-0.244269
	2	0.335912	-0.146622		2	-0.199977	0.370347
	3	-0.357294	0.329038		3	0.304729	-0.107280
	4	0.181841	-0.043826		4	-0.280917	0.157964
	5	-0.123472	0.011041		5	0.079836	-0.008355
	6	0.017992	0.010810		6	-0.032172	-0.011979
	7	0.044440	-0.028232		7	-0.060845	0.041210
	8	0.004457	0.000000		8	-0.004594	-0.000000

Table S6: CASSCF computed Mulliken charges

Atom label	**1**	**1a**	**1b**
O1	-1.3526	-1.3528	-1.3460
O2	-1.3517	-1.3484	-1.3404
O9	-0.5511	-0.5075	–
O8	-0.7660	-0.5089	–
O7	-0.9644	-0.5779	–
O6	-0.7115	-0.4696	–
O5	-0.5932	-0.5478	–

Table S7: SINGLE_ANISO computed spectrum, g tensors, relative energies and angles (q) of the principal anisotropy axes of the first excited states with respect to the ground state, for ground and excited state pseudo doublets of **1a**

Levels	Energy (cm^{-1})	g_{zz}	Δ_{Tun}	Angles between *gzz* axis
1	0.000	19.86	0.001	–
2	0.001			
3	331.605	17.28	0.038	3.44
4	331.643			
5	421.454	18.33	0.841	67.67
6	422.295			
7	434.205	14.78	0.120	27.77
8	434.325			
9	443.359	6.24	–	76.12
10	448.460			
11	453.595			
12	463.155	1.85	–	22.40
13	469.625			
14	475.718			
15	483.788	–	–	–
16	501.760	17.74	2.289	82.48
17	504.049			

Table S8: Composition of wave functions of the ground J = 8 of Ho(III) for complex **1a** as derived from SINGLE_ANISO calculations

w.f.	m_J	c_i		w.f.	m_J	c_i	
		real	imag			real	imag
1	-8	-0.672092	0.218671	2	-8	-0.672093	0.218671
	-7	-0.000825	-0.000159		-7	-0.000825	-0.000161
	-6	-0.001268	-0.017660		-6	-0.001268	-0.017655
	-5	-0.005702	-0.009012		-5	-0.005699	-0.009008
	-4	0.005669	-0.000524		-4	0.005609	-0.000531
	-3	0.001029	0.002733		-3	0.001024	0.002815
	-2	-0.002167	0.001129		-2	-0.002011	0.001084
	-1	-0.000232	0.000118		-1	-0.000195	-0.000108
	0	-0.000057	-0.000357		0	0.000012	-0.000002
	1	-0.000257	-0.000040		1	0.000153	-0.000163
	2	0.002410	0.000404		2	-0.002248	-0.000409
	3	0.000133	-0.002917		3	-0.000103	0.002993
	4	-0.005553	0.001256		4	0.005498	-0.001230
	5	-0.002634	0.010334		5	0.002633	-0.010330
	6	-0.004258	-0.017186		6	0.004257	0.017181
	7	-0.000735	0.000407		7	0.000734	-0.000408
	8	0.706771	0.000000		8	-0.706772	-0.000000
3	-8	-0.000426	0.002232	4	-8	-0.000415	0.002218
	-7	0.006356	-0.703175		-7	0.005129	-0.703370
	-6	0.031365	0.044641		-6	0.031454	0.044719
	-5	0.033526	0.004660		-5	0.032340	0.004277
	-4	0.016795	-0.004121		-4	0.016747	-0.002776
	-3	-0.007696	0.021402		-3	-0.005153	0.020847
	-2	-0.016154	-0.000718		-2	-0.015502	-0.002377
	-1	-0.002004	-0.017137		-1	-0.001343	-0.013529
	0	0.001225	0.001481		0	0.002710	-0.002250
	1	0.016458	0.005178		1	-0.013052	-0.003807
	2	0.002321	-0.016003		2	-0.000513	0.015675
	3	-0.022465	0.003551		3	0.021439	-0.001232
	4	-0.007194	0.015726		4	0.005808	-0.015951
	5	0.001701	-0.033806		5	-0.001742	0.032576
	6	0.037977	0.039171		6	-0.038173	-0.039140
	7	0.691923	0.125452		7	-0.692322	-0.124279
	8	0.002272	0.000000		8	-0.002257	-0.000000
5	-8	-0.003947	-0.001145	6	-8	-0.002119	-0.001118
	-7	-0.013710	0.000749		-7	-0.019354	0.002589
	-6	-0.087159	0.097235		-6	-0.036149	0.080570
	-5	0.008660	0.152546		-5	-0.110082	0.176225
	-4	0.044568	0.367725		-4	0.184236	0.375529
	-3	0.446467	0.197635		-3	0.216225	0.278905
	-2	0.199213	0.005592		-2	0.346929	0.027922

	-1	0.183908	-0.041116		-1	0.113321	-0.094769
	0	0.018418	-0.129606		0	0.107859	0.026706
	1	0.165172	0.090724		1	-0.056011	-0.136695
	2	-0.192884	-0.050129		2	0.319877	0.137177
	3	0.483850	-0.065428		3	-0.321379	0.145795
	4	-0.145249	0.340750		4	0.338171	-0.246182
	5	0.050815	-0.144094		5	0.015140	0.207229
	6	0.056620	0.117667		6	0.005620	-0.088128
	7	-0.012959	-0.004539		7	0.015910	0.011320
	8	0.004110	0.000000		8	-0.002395	0.000000

Table S9: SINGLE_ANISO computed spectrum, g tensors, relative energies and angles (q) of the principal anisotropy axes of the first excited states with respect to the ground state, for ground and excited state pseudo doublets of **1b**

Levels	Energy (cm^{-1})	g_{zz}	Δ_{Tun}	Angles between *gzz* axis
1	0.0	19.89	—	—
2	0.0			
3	528.456	17.28	–	3.43
4	528.456			
5	706.202	15.22	0.002	16.73
6	706.204			
7	763.519	12.40	0.008	2.20
8	763.527			
9	809.502	11.08	0.005	22.94
10	809.507			
11	878.392	7.60	1.150	13.05
12	879.542			
13	965.638	4.88	2.81	7.90
14	968.448			
15	1030.551	–	–	–
16	1056.476	16.32	18.397	89.35
17	1074.873			

Table S10: Composition of wave functions of the ground J = 8 of Ho(III) for complex **1b** as derived from SINGLE_ANISO calculations

w.f.	m_J	c_i		w.f.	m_J	c_i	
		real	imag			real	imag
1	-8	0.501798	-0.497970	2	-8	-0.501803	0.497975
	-7	0.001431	-0.000456		-7	-0.001431	0.000456
	-6	0.006239	0.013319		-6	-0.006239	-0.013320
	-5	-0.000838	-0.000337		-5	0.000838	0.000337
	-4	0.000186	-0.000185		-4	-0.000187	0.000186
	-3	0.000010	0.000103		-3	-0.000009	-0.000103
	-2	0.000007	0.000011		-2	-0.000007	-0.000013
	-1	-0.000011	-0.000003		-1	0.000006	-0.000001
	0	-0.000014	0.000006		0	-0.000002	-0.000004
	1	0.000005	-0.000010		1	0.000005	-0.000004
	2	-0.000003	-0.000013		2	-0.000005	-0.000014
	3	0.000066	0.000080		3	0.000066	0.000080
	4	0.000263	0.000000		4	0.000263	0.000000
	5	0.000357	-0.000829		5	0.000357	-0.000829
	6	-0.004954	-0.013849		6	-0.004954	-0.013849
	7	-0.001337	0.000685		7	-0.001337	0.000685
	8	0.706956	0.000000		8	0.706948	0.000000
3	-8	0.001160	0.001892	4	-8	-0.001160	-0.001892
	-7	-0.349144	-0.611774		-7	0.349144	0.611774
	-6	0.048695	0.022652		-6	-0.048695	-0.022652
	-5	0.029935	-0.005560		-5	-0.029931	0.005559
	-4	-0.002454	0.002902		-4	0.002453	-0.002901
	-3	-0.000368	-0.000706		-3	0.000369	0.000723
	-2	0.000364	0.000090		-2	-0.000339	-0.000072
	-1	0.000076	-0.000022		-1	-0.000027	0.000014
	0	-0.000034	0.000060		0	-0.000002	-0.000001
	1	0.000021	0.000076		1	0.000003	0.000031
	2	-0.000267	-0.000263		2	-0.000238	-0.000252
	3	-0.000795	0.000056		3	-0.000809	0.000063
	4	-0.001192	0.003609		4	-0.001191	0.003607
	5	0.010901	0.028428		5	0.010900	0.028425
	6	-0.044758	-0.029683		6	-0.044758	-0.029683
	7	-0.704049	0.021976		7	-0.704050	0.021976
	8	-0.002219	0.000000		8	-0.002219	0.000000
5	-8	0.008137	-0.011459	6	-8	-0.008137	0.011460
	-7	-0.000293	-0.040109		-7	0.000293	0.040111
	-6	-0.384287	-0.539991		-6	0.384292	0.539996
	-5	0.227355	0.084832		-5	-0.227336	-0.084827
	-4	0.003724	-0.002082		-4	-0.003652	0.002051
	-3	-0.002943	0.003624		-3	0.002962	-0.003689
	-2	-0.000397	-0.000524		-2	0.000382	0.000483

	-1	0.000636	0.000088		-1	-0.000455	-0.000043
	0	0.000006	-0.000003		0	0.000011	0.000022
	1	-0.000297	0.000569		1	-0.000229	0.000396
	2	0.000197	0.000627		2	0.000172	0.000591
	3	0.004659	-0.000302		3	0.004723	-0.000280
	4	0.003854	-0.001831		4	0.003787	-0.001790
	5	-0.062464	0.234489		5	-0.062456	0.234471
	6	0.217792	0.625966		6	0.217794	0.625972
	7	-0.032533	-0.023460		7	-0.032535	-0.023462
	8	0.014055	0.000000		8	0.014055	0.000000

Table S11: SINGLE_ANISO computed spectrum, g tensors, relative energies and angles (q) of the principal anisotropy axes of the first excited states with respect to the ground state, for ground and excited state pseudo doublets of **1c**

Levels	Energy (cm^{-1})	g_{zz}	Δ_{Tun}	Angles between *gzz* axis
1	0.000	19.89	–	–
2	0.000			
3	425.142	17.30	–	0.072
4	425.142			
5	644.085	14.83	–	0.126
6	644.085			
7	761.951	12.37	0.011	0.046
8	761.962			
9	844.001	9.89	0.021	0.259
10	844.022			
11	915.392	7.40	0.544	0.28
12	915.936			
13	978.332	4.92	0.750	0.212
14	978.407			
15	1022.758	2.46	0.313	0.158
16	1023.071			
17	1039.174	–	–	–

Table S12: Composition of wave functions of the ground J = 8 of Ho(III) for complex **1c** as derived from SINGLE_ANISO calculations

w.f.	m_J	c_i		w.f.	m_J	c_i	
		real	imag			real	imag
1	-8	0.427115	0.563534	2	-8	-0.427115	-0.563534
	-7	0.001345	-0.000526		-7	-0.001345	0.000526
	-6	-0.000000	0.000000		-6	0.000000	-0.000000
	-5	0.000005	0.000007		-5	-0.000005	-0.000007
	-4	-0.000000	0.000000		-4	0.000000	-0.000000
	-3	-0.000000	0.000000		-3	0.000000	-0.000000
	-2	0.000029	-0.000003		-2	-0.000028	0.000001
	-1	0.000000	0.000000		-1	0.000000	-0.000000
	0	-0.000000	0.000000		0	-0.000000	-0.000000
	1	0.000000	0.000000		1	0.000000	-0.000000
	2	-0.000015	-0.000025		2	-0.000016	-0.000023
	3	0.000000	-0.000000		3	-0.000000	-0.000000
	4	0.000000	0.000000		4	-0.000000	0.000000
	5	0.000008	-0.000000		5	0.000008	-0.000000
	6	-0.000000	0.000000		6	-0.000000	0.000000
	7	0.000393	0.001390		7	0.000393	0.001390
	8	-0.707105	0.000000		8	-0.707105	0.000000
3	-8	-0.001137	-0.000891	4	-8	-0.001137	-0.000891
	-7	0.571060	-0.416999		-7	0.571059	-0.417000
	-6	0.000000	0.000000		-6	-0.000000	0.000000
	-5	-0.000054	-0.000921		-5	-0.000054	-0.000921
	-4	-0.000000	-0.000000		-4	-0.000000	-0.000000
	-3	-0.000000	-0.000000		-3	-0.000000	-0.000000
	-2	0.000060	0.000086		-2	0.000043	0.000065
	-1	0.000000	-0.000000		-1	0.000000	-0.000000
	0	-0.000000	-0.000000		0	-0.000000	0.000000
	1	-0.000000	-0.000000		1	0.000000	0.000000
	2	0.000101	-0.000031		2	-0.000073	0.000025
	3	0.000000	0.000000		3	-0.000000	-0.000000
	4	-0.000000	-0.000000		4	0.000000	0.000000
	5	0.000610	-0.000692		5	-0.000610	0.000692
	6	0.000000	-0.000000		6	-0.000000	0.000000
	7	-0.192519	-0.680392		7	0.192521	0.680392
	8	-0.001444	0.000000		8	0.001444	-0.000000
5	-8	0.000000	0.000000	6	-8	0.000000	0.000000
	-7	0.000000	-0.000000		-7	0.000000	-0.000000
	-6	0.297095	-0.641664		-6	0.281239	-0.648770
	-5	-0.000000	-0.000000		-5	-0.000000	-0.000000
	-4	-0.000036	-0.001293		-4	-0.000053	-0.001324
	-3	0.000005	-0.000007		-3	-0.000014	0.000043
	-2	-0.000000	-0.000000		-2	0.000000	0.000000

	-1	-0.000098	-0.000098		-1	-0.000131	-0.000129
	0	-0.000227	0.000466		0	0.000007	0.000003
	1	-0.000138	-0.000017		1	0.000183	0.000014
	2	0.000000	0.000000		2	0.000000	-0.000000
	3	-0.000002	0.000008		3	-0.000024	0.000039
	4	0.001041	-0.000767		4	-0.001037	0.000825
	5	-0.000000	0.000000		5	0.000000	-0.000000
	6	0.322895	-0.629076		6	-0.307341	0.636820
	7	0.000000	0.000000		7	-0.000000	-0.000000
	8	-0.000000	0.000000		8	0.000000	0.000000
7	-8	0.000009	-0.000004	8	-8	-0.000009	0.000004
	-7	0.000660	0.000645		-7	-0.000660	-0.000645
	-6	0.000000	0.000000		-6	-0.000000	-0.000000
	-5	-0.689293	0.157718		-5	0.689302	-0.157678
	-4	0.000000	-0.000000		-4	-0.000000	0.000000
	-3	0.000000	0.000000		-3	-0.000000	-0.000000
	-2	0.000025	-0.000048		-2	0.000023	-0.000056
	-1	0.000000	0.000000		-1	0.000000	0.000000
	0	-0.000000	0.000000		0	0.000000	0.000000
	1	-0.000000	0.000000		1	0.000000	-0.000000
	2	0.000041	0.000035		2	-0.000042	-0.000044
	3	-0.000000	0.000000		3	-0.000000	0.000000
	4	0.000000	0.000000		4	0.000000	0.000000
	5	0.698899	-0.107419		5	0.698906	-0.107378
	6	0.000000	-0.000000		6	0.000000	-0.000000
	7	-0.000376	0.000842		7	-0.000376	0.000843
	8	0.000010	0.000000		8	0.000010	0.000000

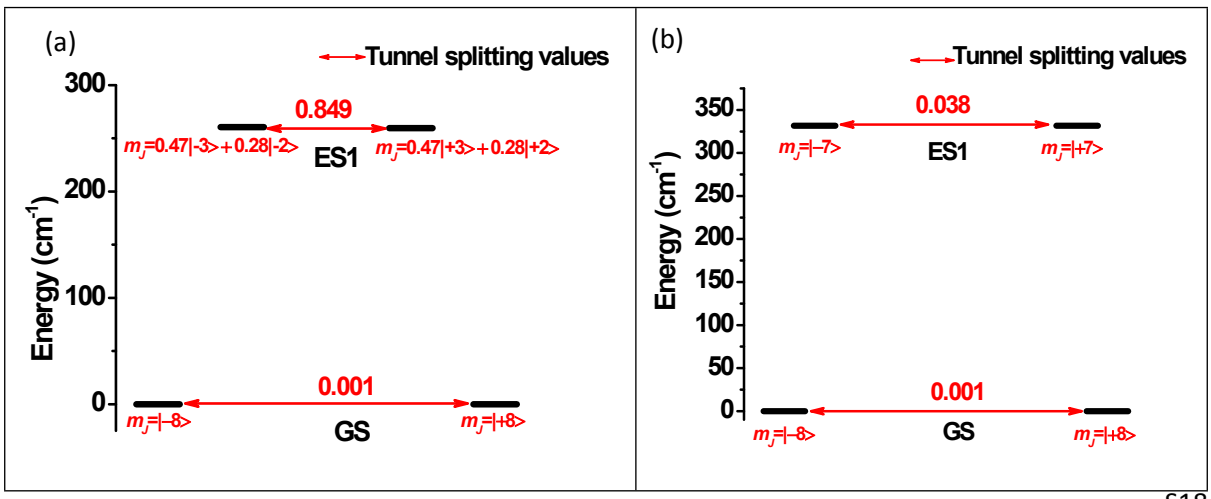

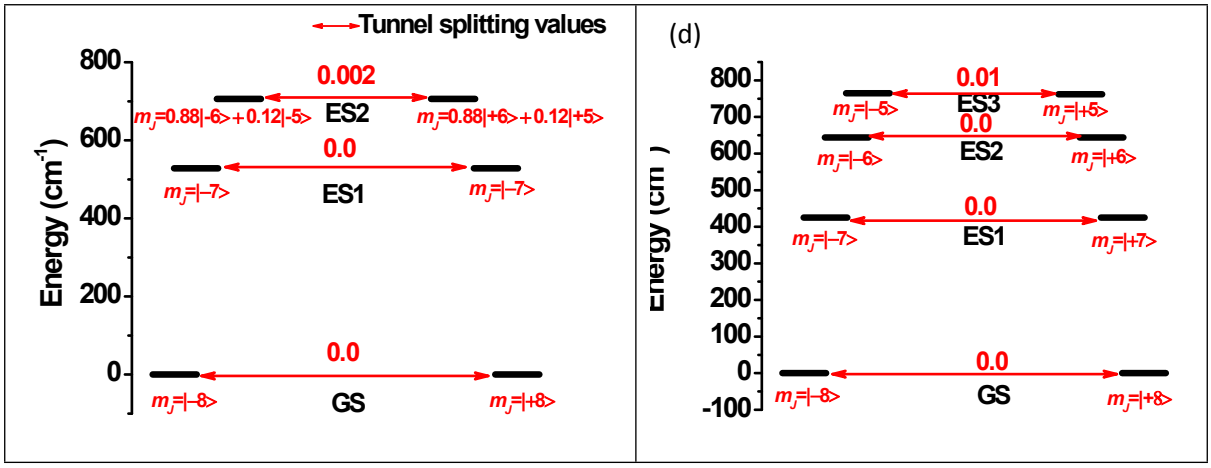

Figure S20: Qualitative mechanism for magnetic relaxation for **1** (a), **1a** (b), **1b** (c) and **1c** (d).

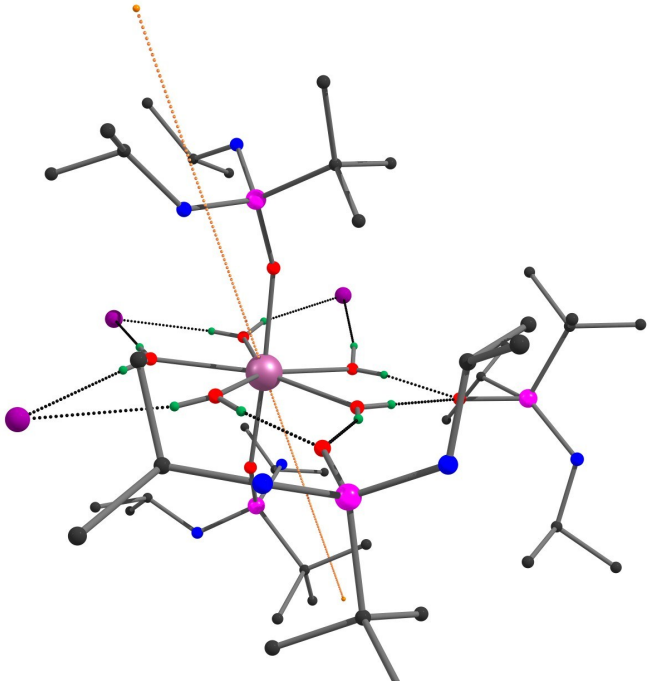

Figure S21: CASSCF computed g_{zz} orientation of the ground state pseudo doublets in **2**.

Table S13: SINGLE_ANISO computed spectrum, g tensors, relative energies and angles (q) of the principal anisotropy axes of the first excited states with respect to the ground state, for ground and excited state pseudo doublets of **2**

Levels	Energy (cm^{-1})	g_{zz}	Δ_{Tun}	Angles between *gzz* axis
1	0.000	16.79	0.021	–
2	0.021			
3	102.602	13.91	0.099	20.95
4	102.701			
5	140.578	17.37	0.102	45.60
6	140.680			

7	247.384	8.75	5.402	32.67
8	252.786			
9	420.007	5.48	8.163	30.70
10	428.170			
11	574.391	2.58	10.512	30.20
12	584.903			
13	645.647	–	–	–

Table S14: Composition of wave functions of the ground *J* = 6 of Tb(III) for complex **2** as derived from SINGLE_ANISO calculations

w.f.	m_J	c_i		w.f.	m_J	c_i	
		real	imag			real	imag
1	-6	0.623511	0.092870	2	-6	0.623570	0.092927
	-5	0.037175	-0.177795		-5	0.037260	-0.177742
	-4	0.237185	0.065035		-4	0.237191	0.064882
	-3	-0.027147	0.089437		-3	-0.027094	0.089071
	-2	-0.015469	-0.010108		-2	-0.016227	-0.009728
	-1	0.001637	0.000809		-1	0.006328	0.000401
	0	-0.000732	0.009877		0	-0.004308	-0.000319
	1	0.001738	-0.000559		1	-0.006318	-0.000536
	2	0.016789	-0.007719		2	-0.017484	0.007230
	3	-0.013675	-0.092460		3	0.013670	0.092092
	4	-0.244178	0.029383		4	0.244163	-0.029212
	5	0.010576	0.181332		5	-0.010654	-0.181293
	6	-0.630390	0.000000		6	0.630456	0.000000

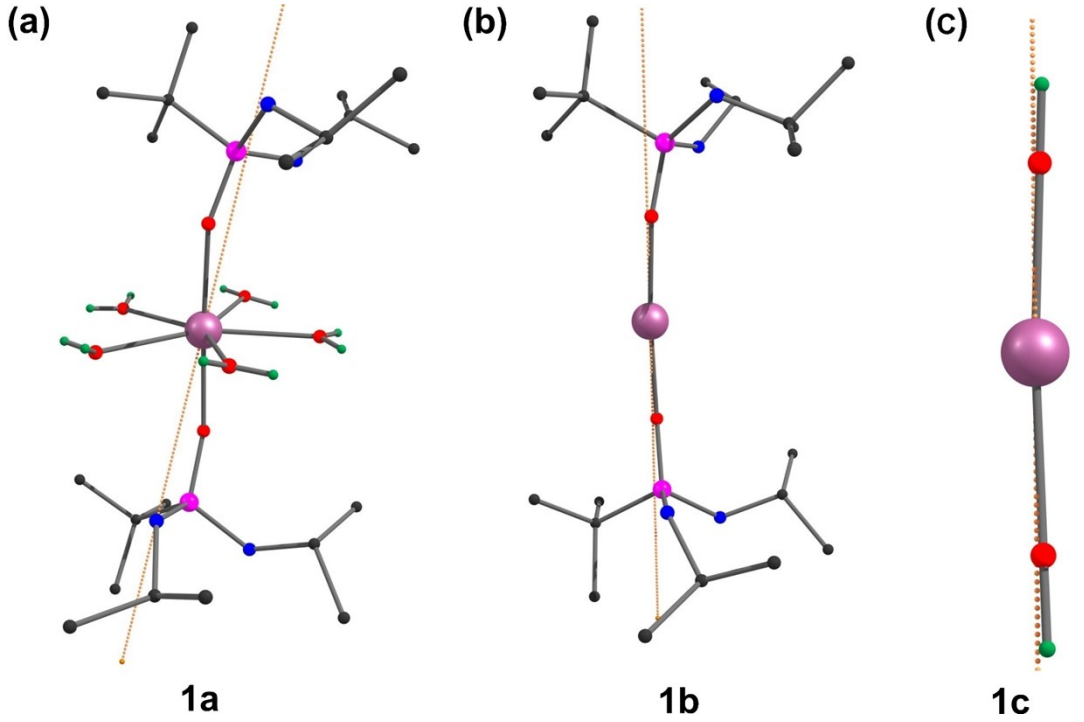

Figure S22: Modelled structures of **2a** (a), **2b** (b) and **2c** (c).

Table S15: CASSCF computed Mulliken charges

Atom label	**2**	**2a**	**2b**
O1	-1.3571	-1.3581	-1.3274
O2	-1.3564	-1.3630	-1.3333
O7	-0.5741	-0.5286	–
O6	-0.6835	-0.4152	–
O5	-0.7752	-0.4002	–
O9	-0.7527	-0.4963	–
O8	-0.5982	-0.5587	–

Table S16: SINGLE_ANISO computed spectrum, g tensors, relative energies and angles (q) of the principal anisotropy axes of the first excited states with respect to the ground state, for ground and excited state pseudo doublets of **2a**

Levels	Energy (cm^{-1})	g_{zz}	Δ_{Tun}	Angles between *gzz* axis
1	0.000	17.89	0.001	–
2	0.001			
3	103.634	15.35	0.011	19.44
4	103.645			
5	266.743	11.74	0.040	18.19
6	266.783			
7	490.941	8.39	6.807	16.96
8	496.748			
9	741.341	5.22	8.030	16.79
10	749.371			
11	957.119	2.38	20.364	17.01
12	977.483			
13	1064.127	–	–	–

Table S17: Composition of wave functions of the ground *J* = 6 of Tb(III) for complex **2a** as derived from SINGLE_ANISO calculations

w.f.	m_J	c_i		w.f.	m_J	c_i	
		real	imag			real	imag
1	-6	0.553525	0.437216	2	-6	-0.553525	-0.437219
	-5	-0.003165	-0.001737		-5	0.003163	0.001728
	-4	-0.039251	-0.027786		-4	0.039240	0.027769
	-3	-0.011022	-0.000813		-3	0.011055	0.000759
	-2	-0.001320	0.001151		-2	0.001371	-0.000893
	-1	-0.000206	0.000576		-1	-0.000014	-0.000468
	0	0.000399	-0.001148		0	-0.000192	-0.000067
	1	0.000196	-0.000580		1	0.000300	-0.000358
	2	0.000322	0.001722		2	0.000523	0.001551
	3	-0.009153	-0.006194		3	-0.009146	-0.006257
	4	0.048024	0.002525		4	0.048005	0.002531
	5	-0.003560	-0.000598		5	-0.003554	-0.000604
	6	-0.705371	0.000000		6	-0.705373	0.000000
3	-6	-0.001441	-0.018863	4	-6	0.001449	0.018849
	-5	-0.114955	-0.660409		-5	0.115082	0.660371
	-4	-0.036972	-0.218012		-4	0.037116	0.218080
	-3	-0.001480	-0.035047		-3	0.001392	0.034864
	-2	0.007244	-0.007529		-2	-0.006992	0.008752
	-1	0.002907	-0.004740		-1	-0.004441	0.003147

	0	0.004323	-0.004665		0	0.000406	0.000376
	1	-0.004505	0.003260		1	-0.002797	0.004669
	2	0.006956	-0.007797		2	0.008191	-0.007642
	3	-0.035057	0.001193		3	-0.034868	0.001284
	4	0.220195	0.020258		4	0.220283	0.020295
	5	-0.667247	-0.064318		5	-0.667248	-0.064140
	6	0.018918	0.000000		6	0.018904	0.000000

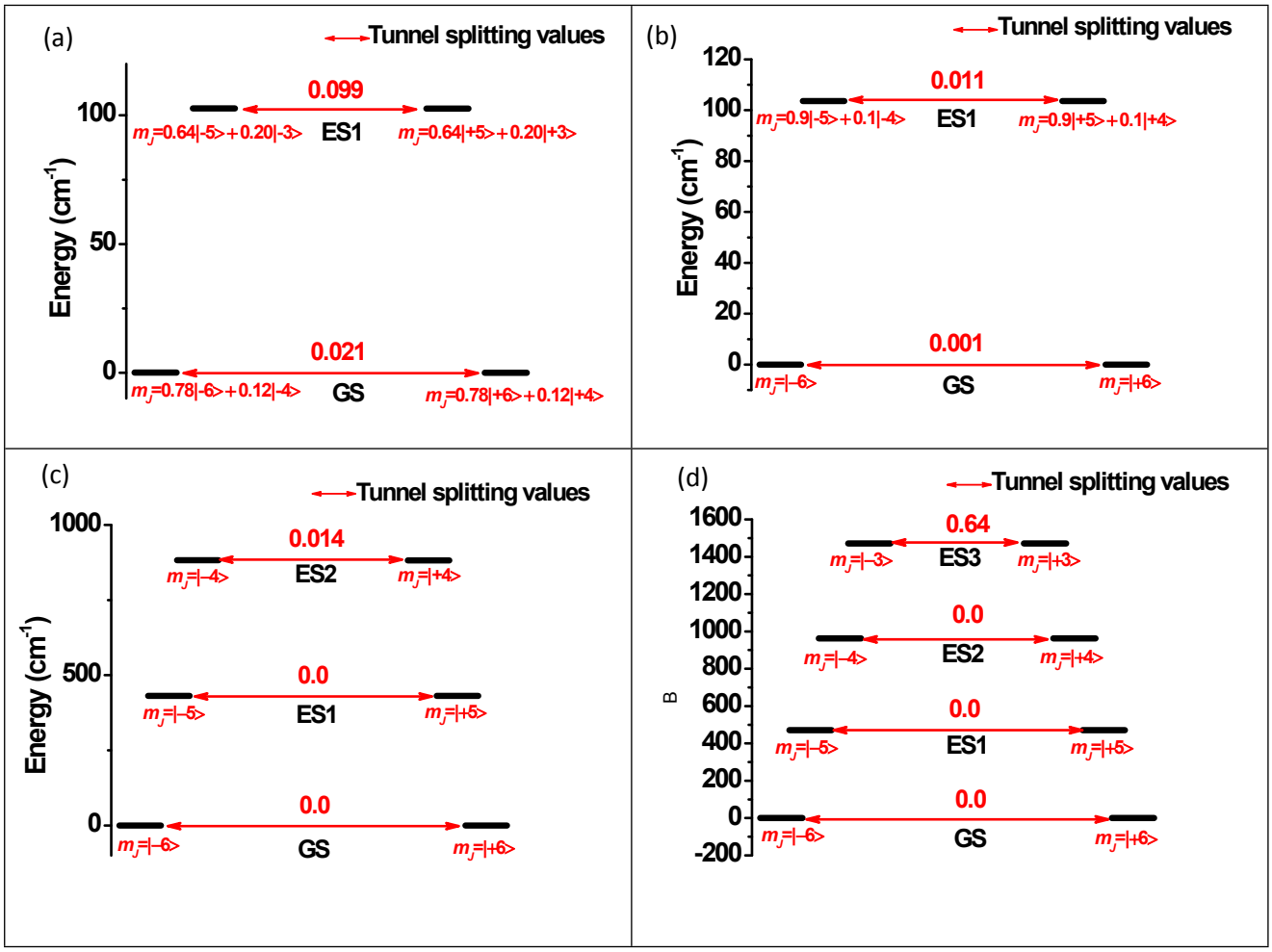

Figure S23: Qualitative mechanism for magnetic relaxation for **2** (a), **2a** (b), **2b** (c) and **2c** (d).

Table S18: SINGLE_ANISO computed spectrum, g tensors, relative energies and angles (q) of the principal anisotropy axes of the first excited states with respect to the ground state, for ground and excited state pseudo doublets of **2b**

Levels	Energy (cm^{-1})	g_{zz}	Δ_{Tun}	Angles between *gzz* axis
1	0.000	17.94	–	–
2	0.000			
3	431.460	14.46	–	0.10
4	431.460			
5	882.318	11.02	0.014	0.39
6	882.332			
7	1350.048	7.65	1.285	0.92
8	1351.333			
9	1823.710	4.42	2.248	2.01
10	1826.138			
11	2224.154	1.67	75.586	4.88
12	2299.740			
13	2480.696	–	–	–

Table S19: Composition of wave functions of the ground *J* = 6 of Tb(III) for complex **2b** as derived from SINGLE_ANISO calculations

w.f.	m_J	c_i		w.f.	m_J	c_i	
		real	imag			real	imag
1	-6	-0.707021	0.010749	2	-6	-0.707021	0.010749
	-5	-0.000055	0.000010		-5	-0.000055	0.000010
	-4	-0.002300	-0.000779		-4	-0.002300	-0.000779
	-3	0.000025	0.000056		-3	0.000025	0.000056
	-2	0.000044	-0.000015		-2	0.000043	-0.000015
	-1	-0.000007	0.000011		-1	-0.000007	0.000012
	0	0.000075	-0.000001		0	0.000000	0.000002
	1	0.000007	0.000011		1	-0.000007	-0.000012
	2	0.000044	0.000015		2	-0.000044	-0.000014
	3	-0.000024	0.000056		3	0.000024	-0.000056
	4	-0.002288	0.000814		4	0.002288	-0.000814
	5	0.000055	0.000010		5	-0.000055	-0.000010
	6	-0.707103	0.000000		6	0.707103	0.000000
3	-6	0.000049	0.000026	4	-6	-0.000049	-0.000026
	-5	-0.657004	-0.261389		-5	0.656985	0.261436
	-4	-0.000644	0.000768		-4	0.000644	-0.000768
	-3	-0.003458	-0.002938		-3	0.003462	0.002936
	-2	-0.000005	0.000133		-2	0.000005	-0.000133
	-1	0.000302	0.000023		-1	0.000023	0.000001

	0	-0.000023	0.000092		0	0.000073	0.000019
	1	0.000277	0.000123		1	-0.000020	-0.000010
	2	-0.000059	0.000119		2	-0.000059	0.000120
	3	-0.004439	0.000940		3	-0.004442	0.000937
	4	0.000202	0.000982		4	0.000201	0.000982
	5	-0.702273	-0.082405		5	-0.702267	-0.082455
	6	-0.000055	0.000000		6	-0.000055	0.000000
5	-6	0.001116	-0.002157	6	-6	0.001116	-0.002157
	-5	0.000865	0.000469		-5	0.000865	0.000469
	-4	-0.516704	0.482640		-4	-0.516733	0.482622
	-3	0.001425	0.002667		-3	0.001426	0.002667
	-2	-0.007020	0.003271		-2	-0.006208	0.002948
	-1	0.000132	0.000084		-1	0.000293	0.000222
	0	-0.000204	-0.000336		0	0.000596	-0.000363
	1	-0.000013	-0.000156		1	0.000062	0.000362
	2	0.006132	-0.004731		2	-0.005472	0.004158
	3	-0.001713	-0.002491		3	0.001713	0.002492
	4	0.666140	-0.237027		4	-0.666159	0.237000
	5	-0.000018	-0.000984		5	0.000018	0.000984
	6	-0.002428	0.000000		6	0.002428	0.000000

Table S20: SINGLE_ANISO computed spectrum, g tensors, relative energies and angles (q) of the principal anisotropy axes of the first excited states with respect to the ground state, for ground and excited state pseudo doublets of **2c**

Levels	Energy (cm^{-1})	g_{zz}	Δ_{Tun}	Angles between *gzz* axis
1	0.000	17.94	–	–
2	0.000			
3	471.463	14.41	–	0.07
4	471.463			
5	962.838	10.92	0.001	0.138
6	962.839			
7	1470.822	7.51	0.635	0.222
8	1471.457			
9	1983.533	4.27	1.791	0.375
10	1985.324			
11	2452.538	1.53	2.664	0.824
12	2455.202			
13	2687.765	–	–	–

Table S21: Composition of wave functions of the ground *J* = 6 of Tb(III) for complex **2c** as derived from SINGLE_ANISO calculations

w.f.	m_J	c_i		w.f.	m_J	c_i	
		real	imag			real	imag
1	-6	0.707060	-0.008166	2	-6	-0.707060	0.008166
	-5	0.000034	0.000087		-5	-0.000034	-0.000087
	-4	0.000000	0.000000		-4	-0.000000	-0.000000
	-3	0.000000	-0.000000		-3	-0.000000	-0.000000
	-2	-0.000016	-0.000026		-2	0.000016	0.000026
	-1	-0.000000	-0.000000		-1	-0.000000	0.000000
	0	0.000034	-0.000000		0	0.000000	0.000000
	1	0.000000	-0.000000		1	-0.000000	-0.000000
	2	-0.000016	0.000026		2	-0.000016	0.000026
	3	-0.000000	-0.000000		3	-0.000000	0.000000
	4	0.000000	-0.000000		4	0.000000	-0.000000
	5	-0.000033	0.000087		5	-0.000033	0.000087
	6	0.707107	-0.000000		6	0.707107	0.000000
3	-6	-0.000080	-0.000048	4	-6	-0.000080	-0.000048
	-5	-0.123463	0.696245		-5	-0.123511	0.696236
	-4	0.000000	0.000000		-4	0.000000	0.000000
	-3	-0.000000	-0.000000		-3	-0.000000	0.000000
	-2	-0.000022	0.000014		-2	-0.000022	0.000014
	-1	-0.000000	-0.000000		-1	-0.000000	-0.000000
	0	0.000011	-0.000040		0	-0.000004	-0.000001
	1	-0.000000	-0.000000		1	0.000000	0.000000
	2	0.000011	0.000023		2	-0.000012	-0.000023
	3	-0.000000	-0.000000		3	0.000000	0.000000
	4	-0.000000	-0.000000		4	0.000000	-0.000000
	5	0.249934	-0.661463		5	-0.249979	0.661446
	6	0.000093	0.000000		6	-0.000093	0.000000
5	-6	0.000000	-0.000000	6	-6	-0.000000	0.000000
	-5	-0.000000	0.000000		-5	0.000000	-0.000000
	-4	-0.260540	-0.657356		-4	0.415814	0.571924
	-3	-0.000758	-0.001255		-3	0.001046	0.001025
	-2	0.000000	0.000000		-2	0.000000	-0.000000
	-1	-0.000046	-0.000019		-1	0.000036	0.000066
	0	-0.000000	0.000000		0	0.000000	0.000000
	1	0.000045	-0.000020		1	-0.000002	-0.000076
	2	0.000000	-0.000000		2	-0.000000	-0.000000
	3	0.000736	-0.001269		3	0.000398	-0.001409
	4	-0.248819	0.661881		4	-0.076421	0.702963
	5	0.000000	0.000000		5	0.000000	0.000000
	6	0.000000	0.000000		6	0.000000	0.000000
7	-6	0.000000	0.000000	8	-6	-0.000000	0.000000
	-5	0.000000	-0.000000		-5	0.000000	0.000000

	-4	0.001460	0.000137		-4	-0.001065	0.001005
	-3	-0.705224	0.051541		-3	0.426942	-0.563665
	-2	-0.000000	-0.000000		-2	0.000000	-0.000000
	-1	-0.000510	-0.000351		-1	-0.000359	0.000634
	0	0.000000	-0.000000		0	-0.000000	0.000000
	1	-0.000592	0.000184		1	0.000686	-0.000244
	2	0.000000	0.000000		2	0.000000	-0.000000
	3	-0.658141	-0.258549		3	-0.628736	0.323556
	4	-0.001435	-0.000303		4	-0.001173	0.000876
	5	0.000000	0.000000		5	0.000000	0.000000
	6	-0.000000	0.000000		6	-0.000000	0.000000